JOURNAL OF MATERIALS SCIENCE 22 (1987) 301–312

Conversion of acrylonitrile-based precursors to carbon fibres

Part 2 *Precursor morphology and thermooxidative stabilization*

MUKESH K. JAIN*, M. BALASUBRAMANIAN, P. DESAI, A. S. ABHIRAMAN‡
Georgia Institute of Technology, Atlanta, Georgia 30332, USA

The progress of stabilization of two compositions of acrylic fibres with various orientations has been followed by a variety of techniques. The thermooxidative treatments for stabilization have been carried out in a continuous process and also in a batch process under free shrinkage, constant length and constant tension conditions. The morphological model of acrylic fibres consists of an alternating sequence of laterally ordered and laterally disordered regions along the fibre direction. This structure is consistent with the observations based on small-angle X-ray scattering of copper-impregnated precursor fibres and thermomechanical response, thermal stress development, calorimetry, wide- and small-angle X-ray scattering and sonic modulus measured at different extents of stabilization. Lateral as well as orientational order in these fibres can be increased markedly through a high-temperature deformation process prior to stabilization. An increase in perfection and extent of order is observed in the early stages of stabilization. There is also a simultaneous decrease in the orientation of the disordered phase at this stage and the extent of this decrease depends on the axial constraints imposed on the fibre. Little difference in the rate of stabilization is observed as measured by density or oxygen uptake for fibres with different extents of orientation, lateral order or restraint. Fibres containing itaconic acid, a stabilization catalyst, did show an increased rate of stabilization. Inferences have been drawn regarding additional research pertaining to achieving high order in precursor fibres, minimizing orientational relaxation during oxidative stabilization, and the techniques for monitoring the extents of the stabilization treatment and the changes in relevant morphological parameters.

1. Introduction

Thermooxidative stabilization constitutes an important intermediate step in the conversion of acrylonitrile-based precursor fibres to carbon fibres. The precursor fibre is transformed at this stage to yield a structure that can be subjected to the high-temperature carbonization treatment without loss of structural cohesion.

It is well known that the properties of the final carbon fibres are determined by a combination of the nature of the precursor fibres and the physical and morphological rearrangements that occur in the stabilization and carbonization steps. Significant changes in morphology and composition occur at each stage. These changes are much affected by the history of thermal treatments as well as the dimensional constraints/stresses imposed during such treatments. Much of the research reported in the literature has been devoted to isolated aspects of the formation of carbon fibres [1] but relatively few attempts have been made to study their development through the stabilization and carbonization stages. Also, the influence of the morphology of the precursor fibres on their stabilization and carbonization behaviour has received little attention. Most of the reported studies involve commercially spun fibres, which restricted them to a limited range of morphology and composition, which were usually unspecified.

A comprehensive experimental facility has been developed in our laboratories to conduct research at all stages of the integrated carbon fibre manufacturing operation. The polymerization and spinning capabilities are an integral part of this research, since they provide the choice of spinning precursor fibres with the desired chemical composition, molecular weight and morphological parameters. We report here the results from a study of the morphology of acrylonitrile-based precursor fibres and the changes introduced in batch and continuous thermooxidative stabilization. The evolution of properties in continuous carbonization is discussed in the third part of this sequence [2]. A comprehensive review of the literature on the physical and morphological changes during the conversion of acrylonitrile-based precursors to carbon fibres is given in Part 1 [1].

2. Experimental procedures

Detailed descriptions of the experimental procedures are given in Jain [3].

**Present address*: ALCAN, Arvida Laboratories and Experimental Engineering Center, Jonquiere, Quebec, Canada.
‡Author to whom all correspondence should be addressed.

0022–2461/87 $03.00 + .12

TABLE I Conditions for spinning of precursor fibres

Precursor	Polymer solution		Coagulation bath		Drawing conditions		Denier/filament
	Concn. (% wt/wt)	Viscosity (P)	Composition (%DMF)	Temperature (° C)	Jet stretch	Draw ratio in boiling H_2O	
I	20	280	60	25	0.7	3	4.1
					0.7	6	2.1
					0.9	3	3.4
					0.7	7.3	1.6
II	17.5	140	60	14	0.7	2.5	3.9
					1.2	3	2.2
					0.7	5	2.2

Spinneret hole diameter was 3 mil (0.003 in.) in all cases.

2.1. Preparation of precursor fibres

Two precursor fibres, I and II, were prepared by solution spinning. For spinning precursor I fibres, a 20% (wt/wt) solution was prepared in dimethyl formamide (DMF) by dissolving commercial acrylic fibres, Orlon 43. For spinning precursor II fibres, a 17.5% (wt/wt) solution of a copolymer of acrylonitrile (AN) and itaconic acid (IA) in the weight ratio of 97/3 (average molecular weight = 131 000 g mol^{-1}, estimated from intrinsic viscosity) was prepared.

The spinning conditions for the two precursors, established to produce fibres of good quality, are given in Table I. The jet stretch and the draw ratio were changed to obtain precursor fibres having different orientations. High-temperature drawing of some of the precursor fibres was performed in order to produce fibres with high orientation and morphological parameters quite different from those produced by drawing in boiling water. Two types of post-spinning high-temperature drawing processes, i.e. hot godet and hot oven, were performed on the hot water (partially) drawn fibres. In the former type of drawing, precursor fibres were drawn directly from the heated feed-godet whereas in the latter type the fibres were first annealed at a relatively low temperature (115 to 130° C) on the feed-godet and then drawn through an oven.

Details of the drawing conditions are given in Table II. The first letter in the sample identification code refers to the precursor type (I for precursor I and II for precursor II). The second and the third terms represent the jet-stretch and the draw ratio (in boiling water), respectively. The last three terms signify the post-spinning, high-temperature plastic drawing conditions such as type of heater (oven or godet), temperature and draw ratio, respectively. The high-temperature draw ratios in these experiments were selected such that the final deniers of the high-temperature drawn fibres matched, within the limits of the experiments, with those of the hot water drawn fibres. This is important if any comparisons in the stabilization and the carbonization behaviour of the two fibres are to be made. The temperatures employed in the hot-oven drawing were the maximum possible for a smooth drawing operation without filament breakages.

2.2. Batch and continuous stabilization

Batch stabilization experiments were carried out in an air circulated oven or in a short tubular furnace, preheated to the desired temperature before the sample was introduced. To determine if dimensional constraints imposed on the fibres influence the changes during this process, experiments were conducted under three different conditions, (i) with free allowance for fibre shrinkage (FL), (ii) by holding the fibre at constant length (CL), and (iii) by hanging suitable weights for constant tension (CT). The batch stabilization treatment was carried out below the temperature at which rapid exothermic stabilization reactions begin.

TABLE II High-temperature drawing conditions

Sample	Draw ratio			Draw godet/ oven temp. (° C)	Annealing godet temp. (° C)	Denier/filament
	B.W.*	H.T.†	Total			
Precursor I						
I-0.9-3-O-252-1.7	3	1.7	5.1	252, oven	130	2.0
I-0.9-3-O-252-2.3	3	2.3	6.9	252, oven	130	1.4
I-0.7-6-O-240-1.2	6	1.2	7.2	240, oven	120	1.7
I-0.7-6-O-240-1.4	6	1.4	8.4	240, oven	120	1.5
Precursor II						
II-0.7-2.5-O-228-1.8	2.5	1.8	4.5	228, oven	115	2.2
II-0.7-2.5-G-160-1.8	2.5	1.8	4.5	160, godet	160	2.2
II-0.7-2.5-O-224-2.5	2.5	2.5	6.2	224, oven	118	1.6
II-0.7-2.5-G-190-2.7	2.5	2.7	6.7	190, godet‡	190	1.5

Sample notation: Precursor type – jet stretch – hot water draw ratio – oven/godet drawing – drawing temperature – draw ratio.
*Draw ratio in boiling water.
†High-temperature draw ratio.
‡The drawn fibres were yellowish due to partial degradation/stabilization.

The tubular furnace for continuous stabilization was divided into three 6 foot (~183 cm) zones with individual temperature controllers for each zone. Smooth transition from one zone to another and the uniformity of temperature throughout a zone were ensured by a metal tube placed between the heaters and the inner glass tube. The temperature profile inside the furnace was determined with thermocouple probes placed 18 in. (~46 cm) apart. Two air pumps, one at each end of the glass tube provided enough air circulation.

Samples for the study of progression of continuous stabilization were obtained after steady state was reached in a constant length run (identical feed and take-up speeds) by cutting the yarn at the delivery end and rapidly pulling it from the feed end. This was then cut into 1 foot (~30.5 cm) sections for subsequent measurements. An apparent residence time for each section was calculated assuming a constant velocity of the yarn from the feed to the exit of the oven. A flat temperature profile of 265° C and feed and take-up velocities of 1 in. min^{-1} (2.54 cm min^{-1}) were employed for this study.

2.3. Thermal analysis

A DuPont DSC model 990 was employed to determine the temperatures at which the precursor fibres undergo exothermic reactions. The analysis was carried out in a regular sample pan at a heating rate of 10° C min^{-1}. The fibres were chopped to small pieces (1 to 2 mm long). The temperature range in which the exotherm was observed was employed as a guide in choosing the stabilization temperatures. Fibres stabilized for various periods were further analysed by this method and the changes in the nature and the extent of exotherms were recorded.

A Perkin Elmer DSC-4 instrument was employed to follow the changes in the heat of melting of fibres, plasticized by water, as a function of the time of stabilization of precursor fibres. The pressure capsules employed in this study were supplied by Perkin-Elmer (Part 319–0218). About 10 mg powdered fibre samples were mixed with water (approximately three times the weight of the fibres). The capsules were carefully sealed, weighed and kept at 50° C for at least 24 h. The melting curves at a heating rate of 10° C min^{-1} were recorded. ΔH_m values per unit mass of fibre samples stabilized for different periods were calculated from the area under the melting curves computed through the Perkin-Elmer data station. The results reported here are to be viewed only for major trends because the degree of reproducibility required for exact quantitative acceptance has not yet been established.

2.4. Wide- and small-angle X-ray scattering

Flat plate wide-angle X-ray diffraction (WAXD) photographs of precursor and batch stabilized fibres were obtained with a Phillips X-ray unit 4100. For quantitative estimation, radial and azimuthal scans were made with a Phillips diffractometer. Samples for equatorial scans were prepared by winding the fibres carefully as a parallel array on the sample holder. The average size of the laterally ordered domains, L_c, also referred to as "crystal size", can be estimated using the Scherrer equation ([4] p. 423):

$$L_c = K\lambda/B_0 \cos\theta \tag{2}$$

where λ is the wavelength of the X-rays, B_0 is the full width at half the maximum intensity (FWHM) in radians and K is a constant commonly assigned a value of unity. The FWHM was estimated from the (1 0 0) peak at $2\theta = 17°$. Corrections to account for inhomogeneous strains and instrumental broadening were neglected in these calculations and so the estimates obtained here are lower bounds for the actual crystal sizes.

Assuming a hexagonal lateral packing of chains in the ordered domains, Herman's orientation function for these segments with respect to the fibre axis, f_c, was calculated from azimuthal intensity scans of the (1 0 0) reflection, $I_{100}(\phi)$. f_c is given by ([4] p. 423)

$$f_c = -2\,\frac{3\langle\cos^2\phi\rangle_{100} - 1}{2} \tag{3}$$

where

$$\langle\cos^2\phi\rangle_{100} = \frac{\int_0^{\pi/2} I_{100}(\phi)\sin\phi\cos^2\phi\,d\phi}{\int_0^{\pi/2} I_{100}(\phi)\sin\phi\,d\phi} \tag{4}$$

where ϕ is the azimuthal angle with respect to the fibre axis direction.

A limited number of small-angle X-ray scattering (SAXS) flat plate photographs of the precursor and the batch stabilized fibres were taken with a Phillips X-ray unit. The study was included to provide a qualitative insight into the macroscopic arrangement of the ordered and the disordered regions in the pristine and the heat-treated fibres. The appearance of a meridional reflection, according to Hess-Kiessig model ([4] p. 334) can be interpreted as an alternating arrangement of the ordered and disordered phases along the fibre axis.

2.5. Sonic modulus

The measurements of sonic velocity through fibre samples were made with the sonic modulus tester PPM-5 by H. M. Morgan Co. Sonic modulus is calculated from sonic velocity, C, measured along the length of the fibre using the following expression:

$$E = \varrho C^2 \tag{5}$$

where E is the modulus and ϱ is the density. When E is expressed in g/denier and C in km sec^{-1}, we obtain,

$$E(\text{g/denier}) = 11.3\,C^2 \tag{6}$$

2.6. Density

Densities of the precursor fibres and fibre samples at different stages of stabilization were measured using the flotation technique using toluene (density = 0.866 g cm^{-3}) and CCl_4 (density = 1.585 g cm^{-3}) mixed together in various proportions to give solutions of densities ranging from 1.11 to 1.55 in steps of 0.01.

2.7. Elemental analysis

Selected samples from the continuous stabilization

line were analysed for carbon, hydrogen and nitrogen (these measurements were made by Atlantic Microlab, Inc., Atlanta, Georgia). Since the stabilized yarn was hygroscopic, it was dried at 80° C and 1 mm mercury pressure for 8 h before the analysis was performed. The oxygen content was calculated by difference, assuming that the only elements present in the precursor and in the stabilized fibres are carbon, hydrogen, nitrogen and oxygen and was plotted as a function of position in the stabilization furnace.

2.8. Shrinkage and shrinkage force

Shrinkage measurements as a function of heating time in batch stabilization under free length were made using an air circulated oven at 265° C. Per cent shrinkage was calculated from the length change, Δl, as $(\Delta l/l)100$ where l is the initial length of the fibre before shrinkage.

Shrinkage force measurements were carried out at constant length by connecting one end of the precursor fibres to an Instron load cell, passing them through a small oven and tying the other end to a rigid support through a Kevlar yarn. The furnace, heated to a predetermined temperature was kept initially on the Kevlar end and then moved quickly over smooth rails to the precursor end. The tension generated in the fibres was recorded as a function of time.

2.9. Mechanical properties

Tensile properties of the fibres were measured with a mini Instron, model 1130 with rubber-faced pneumatic jaws at 50 psi ($\sim 0.35\,N\,mm^{-2}$) air pressure. A gauge length of 10 in. (25.4 cm) and elongation rate of 5 in. min^{-1} (~ 12.7 cm min^{-1}) were employed for testing precursor fibres. Young's moduli of fibres were calculated from the initial slope of the load–elongation curve.

3. Results and discussion

3.1. Summary of results from previous studies in our laboratories

The results from preliminary batch annealing and stabilization experiments with normally drawn precursor I fibres were reported earlier [6]. Significant morphological rearrangements were found to occur both prior to and after the onset of detectable reactions. The degree of changes depended to a large extent on the dimensional constraints imposed during the thermal treatment. The responses indicated clearly the presence of two major phases in the fibres, a laterally ordered phase and a less ordered phase which exhibited a high degree of segmental mobility at temperatures close to those of stabilization. Annealing without dimensional constraints led to a high degree of disorientation in the less ordered phase, with a simultaneous tendency toward increase in both the size and average orientation of the ordered domains. The extent of disorientation in the mobile phase could be reduced significantly by the imposition of dimensional constraints during thermal treatment, indicating that a significant portion of the chain segments in this phase was bridging the ordered domains. The combination of mechanical response and changes in morphological parameters during thermal treatment of these fibres supported the morphological model proposed by Warner *et al.* [6], namely, connected alternating regions of lateral order and disorder (in fibrils), aligned along the fibre direction in oriented acrylic fibres. The results from dimensionally constrained heating also revealed a rapid initial tendency in the precursor fibres toward self ordering, with a significant increase in orientation. This tendency was utilized to improve the orientational and lateral order in the precursor fibres by drawing them at temperatures comparable to those of stabilization.

3.2. Pre-stabilization high-temperature drawing

The properties of high-temperature drawn (HTD) fibres along with the original fibres are given in Tables III and IV. The method of sample designation has been described in the experimental section. The high values of sonic modulus and orientation function, f_c, in HTD fibres suggest a significant increase in the orientation of the ordered phase and in the overall orientation. The average lateral size of the ordered phase (crystal size) increases by more than 100% as a result of this high-temperature drawing. Two samples from precursor I, I-0.9-3-O-252-2.3 (drawn 3 × in hot water followed by an additional 2.3 × in an oven at

TABLE III Properties of precursor I fibres

Sample	Denier/ filament	Tenacity (g/denier)	Elong. (%)	Young's modulus (g/denier)	Sonic modulus (g/denier)	Orientation function, f_c	Crystal size (nm)
First set for preliminary batch-stabilization studies							
I-0.7-3	4.1	1.8	13	61	95	0.54	5.4
I-0.7-6	2.1	2.8	9.5	73	130	0.63	4.7
I-0.7-6-O-250-1.0	2.1	2.5	12	76	145	0.75	10.7
I-0.7-6-O-250-1.2	1.7	3.1	10	111	176	0.79	11.1
I-0.7-6-O-250-1.4	1.5	3.3	8	124	190	0.81	11.5
Second set for batch and continuous stabilization studies							
I-0.7-7.3*	1.6	3.4	11	78	120	0.70	5.4
I-0.9-3	3.4	1.8	19	59	90	0.57	5.1
I-0.9-3-O-252-1.7	2.0	3.2	10	117	175	0.82	12.4
I-0.9-3-O-252-2.3*	1.4	4.1	8	135	211	0.92	13.0

*Fibres chosen for stabilization studies.

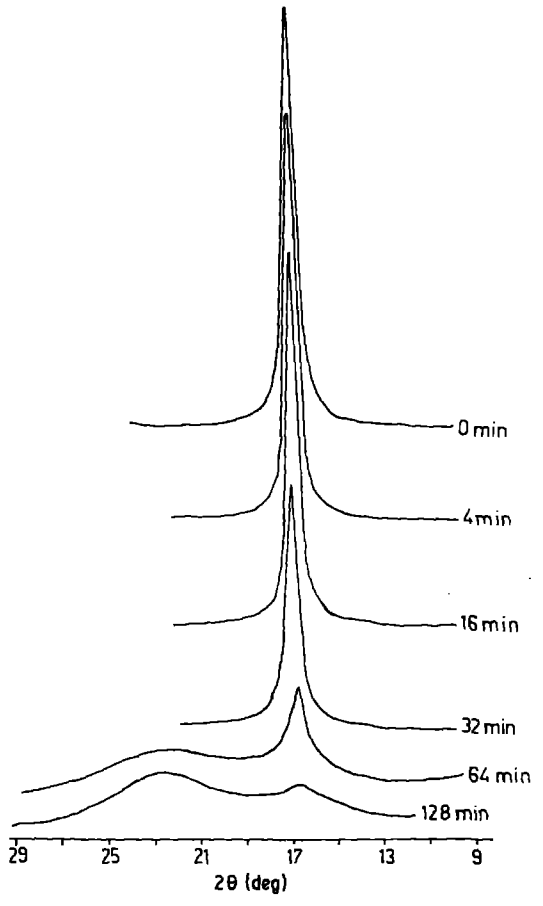

Figure 1 WAXD intensity plots of HTD precursor I fibres heated at 265° C for various durations.

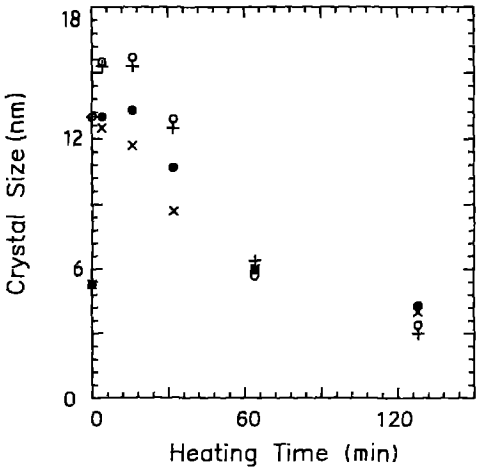

Figure 2 Crystal size of CL and FL batch stabilized fibres. (○) CL, HTD fibres, (●) CL, HWD fibres, (+) FL, HTD fibres, (×) FL, HWD fibres. Heating temperature = 265° C.

252° C) and I-0.7-7.3 (draw ratio = 7.3 in hot water)*, having approximately the same total draw ratio and denier per filament but quite different morphological parameters, were selected to study the influence of orientational and lateral order in the precursor fibres on stabilization.

3.3. Progression of stabilization

3.3.1. Morphological parameters

X-ray diffraction and sonic modulus measurements were made for studying the changes in morphological parameters as a function of stabilization time. Fig. 1 shows a plot of the diffraction intensities against 2θ in a WAXD scan of HTD precursor I fibres heated under constant length conditions at 265° C for various durations. The average size and orientation of the laterally ordered phase in these fibres were estimated as a function of heating time (Figs 2 and 3). The trends are the same as observed before in 3 × and 6 × drawn fibres [5] except that the initial increase in the orientation of the ordered phase is absent in the HTD fibres. Also, the large differences in the crystal size and orientation present in the HTD and HWD fibres diminish as stabilization progresses. The absence of initial increase in orientation of the HTD fibres (Fig. 3) is due to the very high orientation and lateral order that is already present in these precursor fibres.

Orientation of the ordered as well as the disordered phase of the precursor fibres can be inferred from their sonic modulus. High sonic modulus of HTD fibres suggests that there is a high orientation of the ordered and disordered phases along the fibre axis direction. A continuous decrease in this orientation in HTD fibres is observed during their stabilization (Fig. 4), even when no macroscopic shrinkage is allowed. This behaviour is different from the response of the HWD fibres, where an initial increase in sonic modulus at short heating times, followed by a continuous decrease at longer times, is observed. The absence of any further increase in order in HTD fibres could be attributed again to the already high overall orientation present in these fibres. Possible relaxation of some segments in the disordered phase which are

TABLE IV Properties of precursor II fibres

Sample	Denier/ filament	Tenacity (g/denier)	Elong. (%)	Young's modulus (g/denier)	Sonic modulus (g/denier)	Orientation function, f_c	Crystal size (nm)	Density ($g\,cm^{-3}$)	Moisture content (%)
Boiling water drawn fibres									
II-1.2-3	2.2	2.1	11.1	78	95	0.67	7.3	1.180	2.1
II-0.7-5	2.2	3.1	11.8	90	149	0.78	7.5	1.175	2.0
II-0.7-2.5	3.9	1.8	11.4	64	105	0.61	6.5	–	–
High-temperature drawn fibres									
II-0.7-2.5-O-228-1.8	2.2	3.4	9.7	114	150	0.83	11.3	1.175	1.8
II-0.7-2.5-G-160-1.8	2.2	3.5	8.6	117	147	0.77	8.8	1.175	1.7
II-0.7-2.5-O-224-2.5	1.6	4.4	8.7	132	182	0.87	11.0	1.180	2.1
II-0.7-2.5-G-190-2.7	1.5	4.4	7.6	144	207	0.84	12.8	1.185	1.6

*Referred to as HTD and HWD fibres, respectively, in all subsequent discussions.

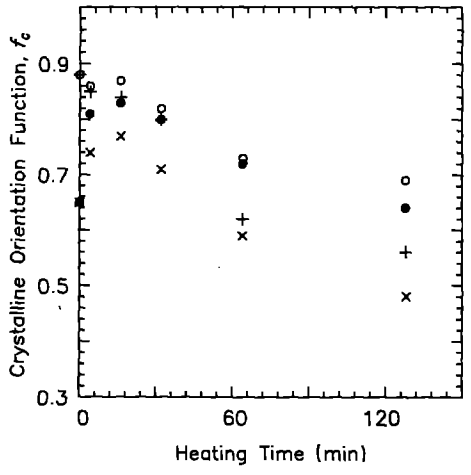

Figure 3 Crystalline orientation function, f_c, of CL and FL batch stabilized fibres. (o) CL, HTD fibres, (●) CL, HWD fibres, (+) FL, HTD fibres, (×) FL, HWD fibres. Heating temperature = 265° C.

not anchored effectively in the ordered phase may contribute to a decrease in the sonic modulus even at short heating times in these fibres. This partial relaxation of orientation in the disordered phase is also suggested by the shrinkage force experiments discussed in Section 3.3.3 (a part of the initial stress developed relaxes almost instantaneously). In HWD fibres, an increase in the sonic modulus is observed at short heating times in spite of probable partial relaxation in the less ordered phase, because of the simultaneous large increase in the crystalline orientation (Fig. 3). The decrease in sonic modulus at longer heating periods is due to the change in the intrinsic properties of the precursor fibres as a result of stabilization reactions. As expected, the free length heated fibres show a pronounced decrease in the sonic modulus in both precursor fibres (Fig. 4), due to the extensive orientational relaxation of even the bridging segments in the disordered phase between the ordered domains. In constant tension experiments, with the applied tension being the maximum that was possible without causing filament rupture, the fibres extended by almost 10 to 12%. This extension caused an increase in orientation in both HTD and HWD fibres, as reflected by the initial increase in sonic modulus (Fig. 4). The rise in sonic modulus, as expected, is more pronounced in the case of the HWD fibres.

The sonic moduli of samples from a continuous stabilization line are plotted in Fig. 5 as a function of residence time in the oven (apparent heating time). The sampling technique has been described in the experimental section. Although continuous stabilization was carried out at the same feed and take-up speeds, it does not prevent local changes in the velocities due to compensating extension and shrinkage of the fibre inside the furnace. The fibre, as soon as it reaches a temperature above its glass transition temperature (T_g), will tend to shrink provided the shrinkage can be compensated by extension in another section of the furnace. Warner *et al.* [7] have explained this phenomenon in detail. The general trends in the sonic moduli of both HWD and HTD fibres observed in continuous stabilization are similar to those in batch stabilization at constant length (Fig. 4). The slower initial increase in the sonic modulus of HWD fibres in continuous stabilization when compared to batch stabilization is due to a slower heating to 265° C in the former as opposed to the instantaneous exposure to 265° C in the latter process.

3.3.2. Calorimetry

The DSC exotherms of samples from a continuous stabilization run, representing various apparent heating periods, are shown in Fig. 6. A simultaneous decrease in the area under the exothermic peak and increase in the peak width are observed. As stabilization progresses, the nitrile groups in the precursor fibre undergo cyclization resulting in a decrease in the extent of the exotherm. A complete disappearance of the exotherm suggests completion of the cyclization reactions. Incorporation of oxygen and cyclization of nitrile groups during the stabilization of precursor fibre alters the chemical structure originally present in these fibres. This new structure formed during the intermediate stages of stabilization modifies the course of further cyclization, as indicated by the broadening of the exothermic peak.

The results from plasticized melting studies are

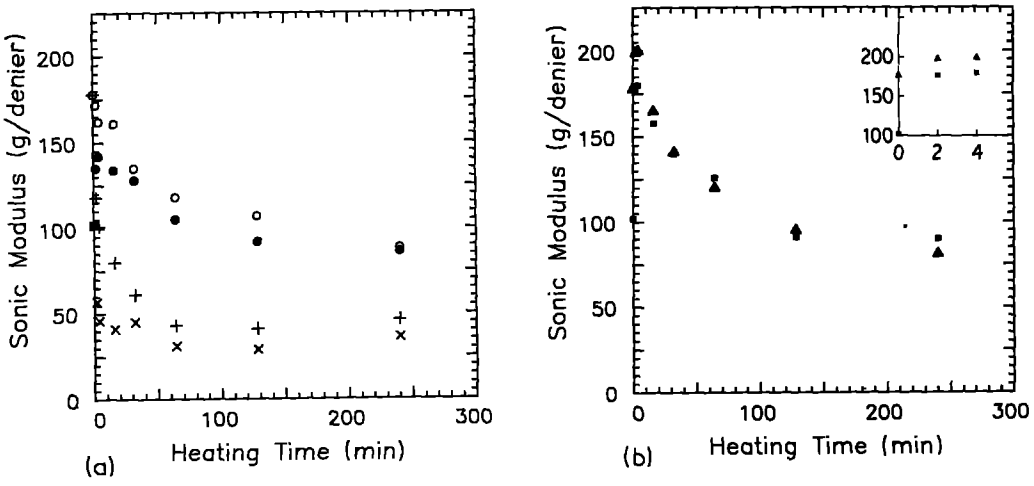

Figure 4 Sonic modulus of CL, FL and CT batch stabilized fibres. (a): (o) CL, HTD fibres, (●) CL, HWD fibres, (+) FL, HTD fibres, (×) FL, HWD fibres. (b): (■) HWD fibres, 0.1 g/denier tension; (▲) HTD fibres, 0.14 g/denier tension. (Inset: the initial response,plotted on an expanded scale.) Heating temperatures = 265° C.

TABLE V Results of plasticized melting studies

Heating time (min)	HTD fibres				HWD fibres			
	Heat of melting ($cal\,g^{-1}$)	$\Delta H_m(t)/\Delta H_m(t=0)$	Heat of crystallization ($cal\,g^{-1}$)	$\Delta H_c(t)/\Delta H_c(t=0)$	Heat of melting ($cal\,g^{-1}$)	$\Delta H_m(t)/\Delta H_m(t=0)$	Heat of crystallization ($cal\,g^{-1}$)	$\Delta H_c(t)/\Delta H_c(t=0)$
0	12.3	1.00	9.51	1.00	12.9	1.00	9.45	1.00
2	12.5	1.02	9.81	1.03	12.0	0.93	9.07	0.96
4	12.3	1.00	9.68	1.02	13.4	1.04	8.96	0.95
16	16.5	1.34	9.46	0.99	10.3	0.80	7.10	0.75
32	9.2	0.75	4.68	0.49	7.6	0.59	4.39	0.46
64	1.9	0.15	–	–	Negl.	–	Negl.	–

Temperature of heating = 265° C.

given in Table V. Depletion of the unreacted ordered phase in the later stages of the process can be seen clearly, consistent with the WAXD results reported earlier. Plasticized recrystallization results show the expected monotonic decrease in the potential of the material to crystallize with increasing time of thermal treatment. The most important aspect of these plasticized melting and recrystallization experiments is the clear observation of the characteristic enthalpy changes associated with first order transitions, establishing the presence of true crystals in the precursor fibres.

3.3.3. Shrinkage and shrinkage force

Shrinkage in acrylic fibres during their stabilization has been employed for the optimization of stabilization by previous researchers [8]. Total shrinkage during stabilization under free conditions can be divided into an almost instantaneous initial shrinkage due to the coiling-up of the oriented chains in the laterally disordered phase and a slow delayed shrinkage, also known as secondary shrinkage, which has been attributed to the chemical reaction associated with stabilization [9–11]. A plot of shrinkage against heating time, with the fibres heated at 265° C in air, is given in Fig. 7. The HTD fibres shrink instantaneously to a lower extent, 12%, compared to HWD fibres which show an instantaneous shrinkage of 17%, the difference being maintained throughout the stabilization process. The lower entropic shrinkage in HTD fibres is due to the presence of a higher fraction of the laterally ordered phase and thus a lower fraction of the oriented but laterally disordered regions which contribute to this shrinkage. The secondary shrinkage which increases with the progression of stabilization is caused by the chemical reactions associated with the stabilization. Melting of the ordered segments which takes place during the course of chemical reactions can result in continued shrinkage with the progression of stabilization. Both HWD and HTD fibres show similar rates and extents of secondary shrinkage.

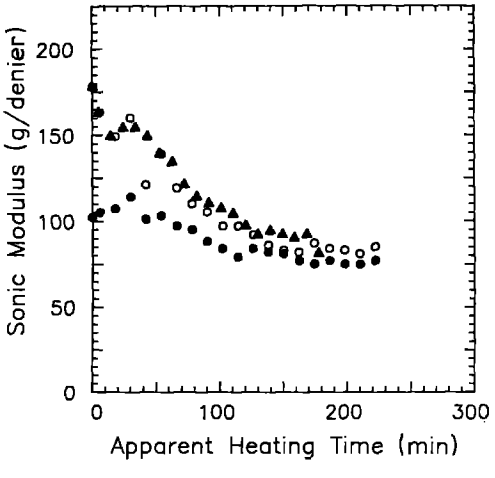

Figure 5 Change in sonic modulus during continuous stabilization at 265° C. (●) HWD fibres, 1 in. min^{-1}, (○) HTD fibres, 1 in. min^{-1}, (▲) HTD fibres, 1.25 in. min^{-1}.

When no macroscopic changes in the length of precursor fibres are allowed during heating, stress is developed due to the tendency of chains in the disordered phase to undergo entropic relaxation. This tendency of the chains to coil up is greater when their orientation is higher. Fig. 8 shows the stress or shrinkage force generated in the HTD and HWD fibres as a function of heating time. The HTD fibres have a significantly higher non-crystalline and overall orientation compared to the HWD fibres and therefore show a higher shrinkage force. Much of the initial tension decays in a relatively short period (less than 2 min) due to relaxation of some of the oriented chains in the disordered phase. The decay is slower and to a lower extent in HTD fibres compared to HWD fibres, suggesting higher connectivity between the ordered and the disordered phases. Under a macroscopically constrained state, the chains in the disordered phase of the HTD fibres cannot relax as much as the chains in HWD fibres, in spite of a larger tendency toward it.

The dependence of shrinkage force on the draw ratio is shown in Fig. 9 where the initial stresses generated in three precursor fibres having different draw ratios are plotted. An almost instantaneous and complete decay of the initial stress is observed in fibres with no high-temperature drawing, whereas fibres with high-temperature draw ratios of 1.7 and 2.3 show a larger initial stress and a slower decay, again suggesting a higher connectivity between the ordered and the disordered segments in these highly ordered fibres. The decay of initial stress is followed by a slow development of a secondary stress as a result of chemical reactions propagating to the ordered regions. As discussed earlier, these reactions are accompanid by the melting of the ordered domains which results in the development of a shrinkage force in the later stages of stabilization. Consistent with the extents of lateral order in the precursor fibres, a higher secondary stress is observed in the HTD fibres than in HWD fibres.

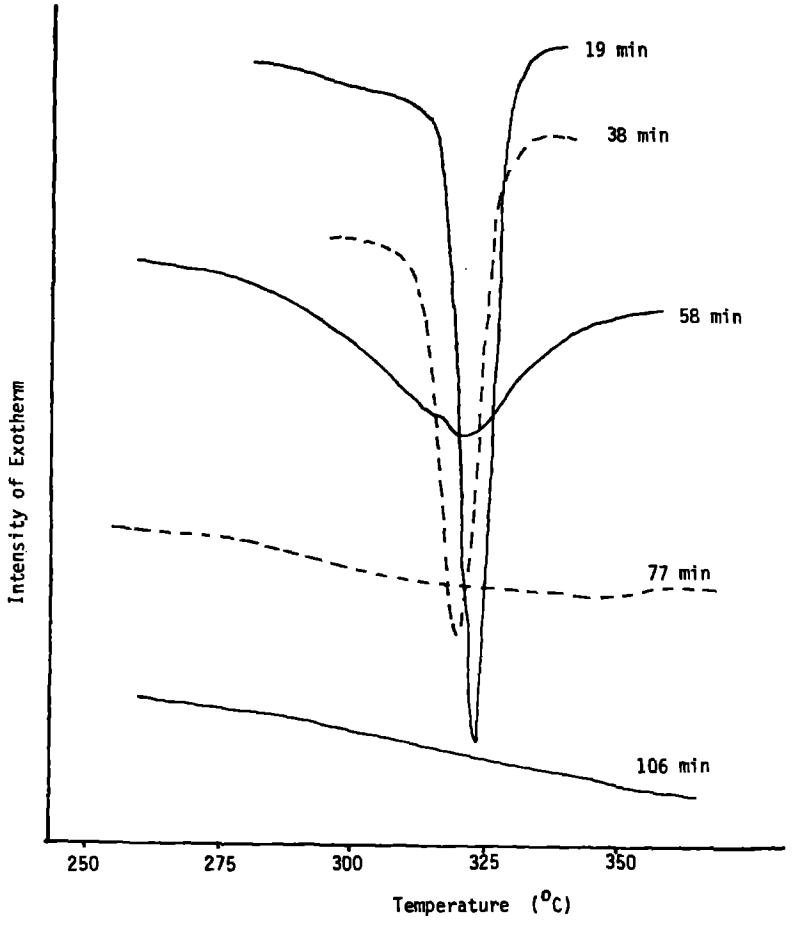

Figure 6 DSC exotherms of samples from continuous stabilization (265° C, flat profile). Various apparent heating times are shown for precursor I-0.9-3-O-252-1.7.

3.3.4. Density and oxygen pick-up

Incorporation of oxygen from the air and the denser packing of the aromatic species created during stabilization contribute to a monotonic increase in density. Both density and oxygen content have been employed in the industry as indicators of the extent of stabilization in acrylic fibres and this aspect is discussed in Part 3 [2]. The progressions of densities of the HTD and HWD precursor I fibres during batch and continuous stabilization are shown in Figs 10 and 11. Under each condition of dimensional constraint imposed during this process (FL, CL, CT or continuous), little difference is seen between the rates of change in HTD or HWD fibres. Although significant differences exist in the morphological parameters of these two precursor fibres (Table III), these differences diminish due to the rearrangements in the early stages of stabilization (Figs 2 to 5). Thus morphological contributions to the rates of solid-state reactions in stabilization, as inferred by density changes, are not likely to be revealed here. The diffusion-controlled incorporation of oxygen (Fig. 12) is also entirely consistent with the progression of density. The rate of stabilization increases with the tension (Fig. 10) in the fibres (tension in free length < in constant length < in constant tension). This, however, can not be attributed unequivocally to the higher orientations obtained at the higher tensions. The filament diameter also decreases with increase in the tension, thus raising the overall rate of diffusion-controlled reactions.

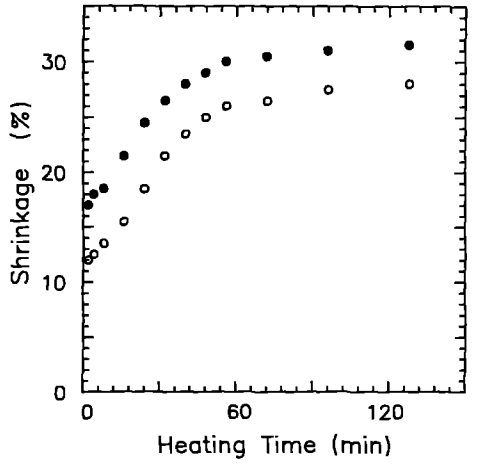

Figure 7 Shrinkage in FL batch stabilized fibres. (○) HTD fibres, (●) HWD fibres. Temperature = 265° C.

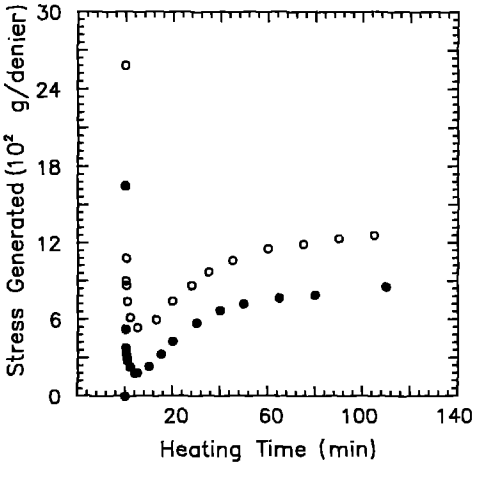

Figure 8 Shrinkage stress generated during CL batch stabilization. (○) HTD fibres, (●) HWD fibres. Temperature = 265° C.

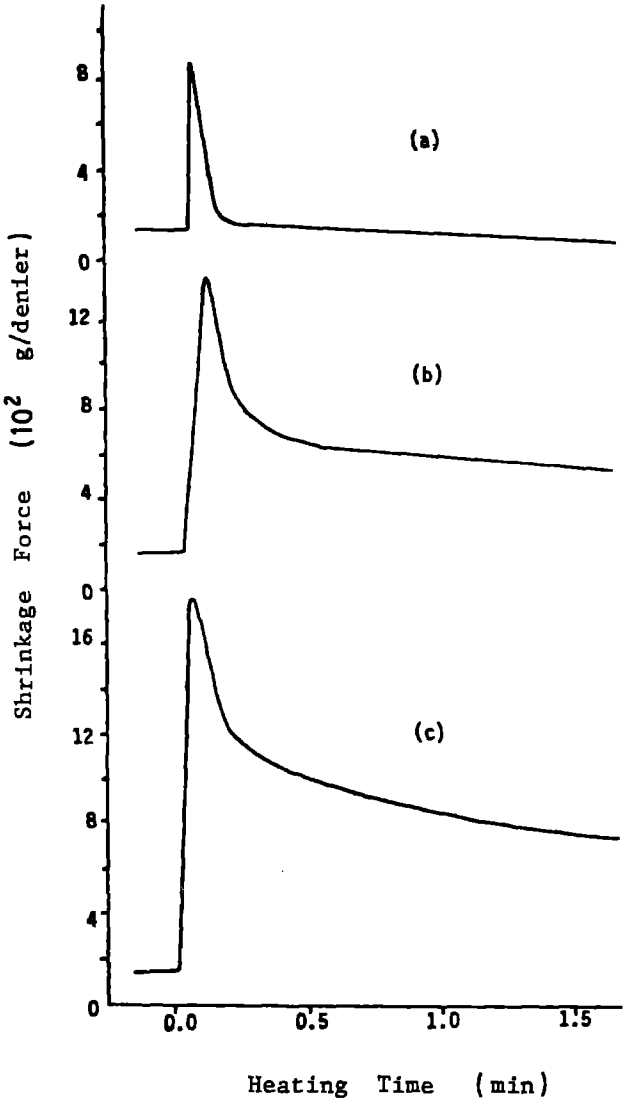

Figure 9 Shrinkage stress generation and decay in precursor I fibres. (a) I-0.9-3, (b) I-0.9-3-O-252-1.7, (c) I-0.9-3-O-252-2.3.

3.3.5. Comparison of precursors I and II

The progression of changes observed in batch and continuous stabilization of precursor II fibres, containing itaconic acid comonomer which can initiate the stabilization reactions, has the same general character as those reported here for precursor I fibres. The quantitative differences observed are due to the higher rate of stabilization in precursor II fibres. For example, the density changes (Fig. 13) for two precursor fibres (I-0.7-7.3 and II-0.7-5) show a significantly higher rate of increase in precursor II in spite of the higher denier of these filaments (2.2 denier) when compared with the denier of the precursor I filaments (1.6 denier). When these fibres are heated at constant length, the delayed shrinkage force, which indicates the propagation of stabilization reactions, also rises much faster in precursor II fibres, suggesting a higher rate of stabilization in these fibres (Fig. 14). Additional results from stabilization of this precursor are reported in Part 3 [2].

3.4. Morphology of acrylic precursor fibres

The following observations clearly show that the basic morphological unit in oriented acrylic fibres consists of a repeating sequence of oriented, laterally ordered and oriented but laterally disordered domains with a significant portion of the chain segments in the latter phase bridging the ordered domains. This model has been proposed earlier by Warner *et al.* [6]:

1. clear WAXD evidence for the presence of laterally ordered domains;
2. calorimetric evidence for the "melting of crystals" when the melting temperature is reduced through plasticization to temperatures below those of degradation reactions;
3. spontaneous shrinkage at high temperatures, *without any loss in the extent or the orientation of the ordered domains*, and the large drop in sonic modulus which accompanies this shrinkage process indicating that the ordered and disordered domains are arranged in a connected sequence along the fibre direction;
4. when thermal treatment of oriented acrylic fibres is carried out without allowance for shrinkage, the change in sonic modulus depends on the change in the extent of lateral order in the fibres. An increase in sonic modulus accompanies a significant initial increase in the extent and orientation of the laterally ordered fraction but a measurable decrease is seen when only a slight increase in lateral order occurs in those fibres which possess a high degree of initial order. These responses indicate the presence of *celia* and loose loops in the laterally disordered fraction.

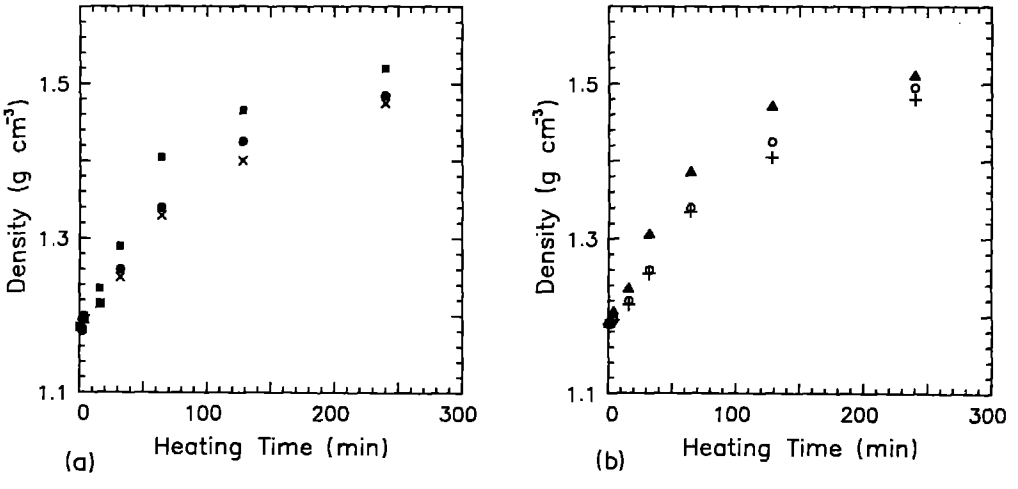

Figure 10 Effect of constraints on the density of batch stabilized HWD and HTD fibres. (a): HWD fibres, (×) FL, (●) CL, (■) 0.1 g/denier tension. (b): HTD fibres, (+) FL, (○) CL, (▲) 0.14 g/denier tension. Temperatures = 265° C.

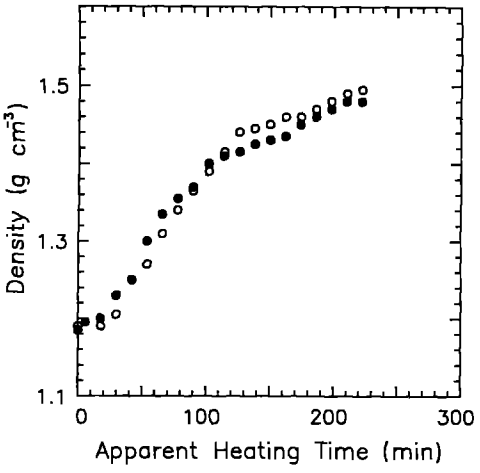

Figure 11 Change in density during continuous stabilization at 265° C. (●) HWD fibres, (○) HTD fibres.

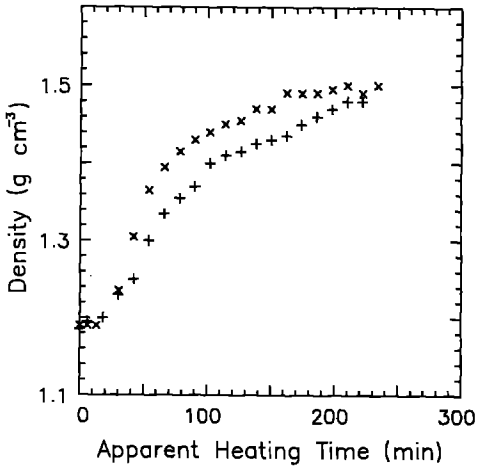

Figure 13 Change in density of precursor I and II fibres during continuous stabilization at 265° C. (+) I-0.7-7.3, (×) II-0.7-5.

The initial decrease in sonic modulus during "constant length" heating of HTD fibres is still much less than the drastic drop which accompanies "free" thermal treatment, indicating that a majority of the segments in the laterally disordered fraction act as tie chains between the laterally ordered domains;

5. acrylic fibres with demonstrably different extents of order show little difference in density, indicating that the packing densities in the laterally ordered crystals and the laterally disordered "noncrystalline" regions are essentially the same. Thus, the meridional reflection in SAXS, characteristic of the proposed two-phase oriented structure, is absent in these fibres (Fig. 15a). After heating the precursor fibres for 16 min in air, a meridional spot is observed in SAXS flat plate photographs, indicating the presence of a long period (Fig. 15b). Appearance of this meridional reflection with the onset of stabilization reactions has been presumed to be the result of their preferential occurrence in one of the two phases, thus providing indirect evidence for the proposed morphology. Confirmation of the existence of a long period in the precursor fibres is obtained by conducting SAXS studies subsequent to impregnation of these fibres with copper ions (Fig. 15c) by refluxing them in a solution of CuCl in HCl for 30 min. The electron density of the disordered phase is increased by the dispersion of copper salt in this phase, resulting in the appearance of the meridional reflection in SAXS studies.

4. Conclusions

A number of significant results have been obtained through the research on oxidative stabilization of acrylic precursors for carbon fibres reported here. These results and the inferences from them regarding needed additional research are summarized below.

1. Through a combination of evidence from thermomechanical response, thermal stress development, calorimetry, wide-angle and small-angle X-ray scattering, and sonic modulus studies of fibres through the course of an oxidative stabilization process, and small-angle X-ray scattering studies of precursor fibres impregnated with copper, the basic morphological unit in oriented acrylic fibres has been shown to have laterally ordered domains connected along the fibre axis direction through domains in which such order is absent. Our observations confirm this important aspect of the morphological model proposed by Warner *et al.* [6]. The other major aspect of their model, fibrillar geometry of this morphological unit, is being examined through small- and wide-angle X-ray

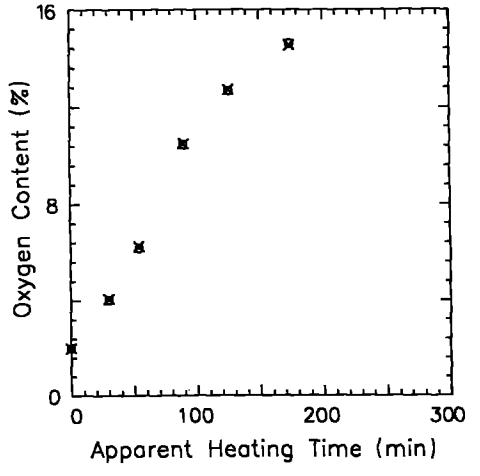

Figure 12 Oxygen incorporation during continuous stabilization of precursor I fibres at 265° C. (×) HWD fibres, (○) HTD fibres.

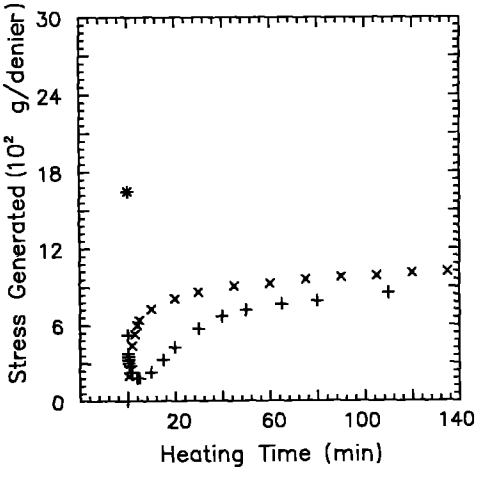

Figure 14 Shrinkage stress developed in precursor I and II fibres at 265° C. (+) I-0.7-7.3, (×) II-0.7-5.

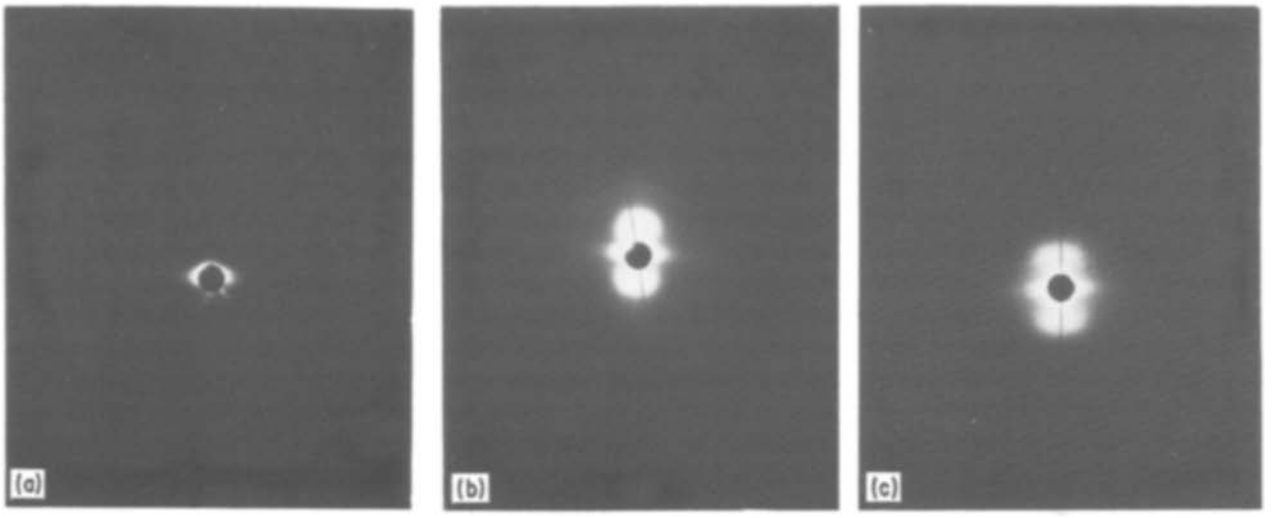

Figure 15 Small-angle flat plate photographs: (a) precursor, (b) 16 min CL stabilized, (c) copper impregnated.

scattering studies of oriented acrylic fibres after swelling them in DMF.

2. The ordered fraction and the overall orientational order in acrylic precursor fibres can be increased markedly through a process which involves plastic stretching at high temperatures of a fibre which has been only partially stretched in a conventional wet spinning process.

3. When acrylic precursor fibres are heated to the temperatures involved in the oxidative stabilization step of the process for carbon fibre formation, the physical changes that precede the onset of a significant level of stabilization reactions depend on the externally imposed dimensional constraints. The present study shows clearly that whether dimensional constraints are imposed or not, a significant tendency for increase in perfection and the extent of the laterally ordered domains occurs in the early stages of this step. The extent of this increase diminishes with increasing order initially present in these fibres. The constraints imposed on the length have a pronounced effect on the relaxation of orientation in the laterally disordered fraction. The decrease in orientation in this phase is dramatic when no constraint against shrinkage is imposed on the fibres. The effect of the degree of orientational relaxation permitted at this stage, which can be controlled by the application of stress, on the ultimate properties of carbon fibres produced from these fibres remains to be studied.

4. The critical stress for failure and the stresses generated at any level of imposed deformation (or, conversely, the deformation at any level of imposed stress) would change throughout the course of stabilization. Since the temperature–tension/deformation–time profile that can be applied during stabilization is limited by the continuously changing critical stress, it is necessary to have the provision to control these through a multistage stabilization process so that the influence of these factors on the structure of the carbon fibres can be established. There is a clear need for separating the stabilization process into at least three independently controlled stages, i.e. an initial zone of rapid morphological rearrangements, a second zone of reactions predominantly in the disordered fraction, and the subsequent zone of reactions propagating into the ordered fraction of the fibres. A multistage stabilization line would also allow the use of different environments in the different zones. In order to realize the maximum potential of a given precursor fibre, it is important to "tailor" the conditions of oxidative stabilization to suit the rates of such reactions and the deformation characteristics of the fibres during this stage. Conducting precisely controlled experiments at this stage will help in establishing the important link between the structure of the precursor fibres and the structure and properties of the carbon fibres that can be obtained from them.

5. When the progression of stabilization is monitored with measurements such as density and oxygen pick-up, little difference is seen in the rates of stabilization with the orientation or the lateral order present initially in the fibres. This appears to be the result of the nature of morphological rearrangements during the early stages of the process, especially the increase in the extent of the ordered fraction to approximately the same levels in these fibres.

6. Among the techniques examined in the present study for the characterization of morphological parameters of the fibres, wide-angle X-ray diffraction (WAXD), sonic modulus, differential scanning calorimetry (DSC), birefringence and infrared dichroic ratio, the combination of sonic modulus, WAXD and DSC was found best suited for obtaining at least semi-quantitative measures of the degree of lateral order and orientation in the precursor fibres and the changes occurring in the early stages of stabilization. Birefringence and infrared dichroic ratio were discarded because of apparently similar polarizabilities parallel and perpendicular to the chains at the precursor stage which render them unsuitable for distinguishing differences in orientational order. The difference in intrinsic polarizabilities parallel and perpendicular to the chain direction is known to become significant when these fibres are subjected to the conditions of a stabilization process. Infrared dichroism and birefringence may prove suitable for inferring the orientational order in stabilized fibres.

7. During the early stages of a stabilization process,

at least partial relaxation of orientation occurs in the occurs in the fraction in which lateral order is absent, even when a macroscopic constraint against shrinkage is present. These disorienting segments to which macroscopic constraints are not transmitted could be one of the sources of sites of low orientational order and structural defects in carbon fibres. The degree to which it can be eliminated through increase in order in the precursor fibres and through a significant increase in the molecular weight of the precursor polymer remains to be explored.

8. Aspects related to the extent to which the stabilization reactions need to be carried out before the fibres would become suitable for carbonization are discussed in Part 3 [2].

Acknowledgements

We wish to thank Dr L. H. Peebles for many useful suggestions during the course of this work and in the inferences drawn from experimental data. Discussions with Dr W. C. Tincher and Dr F. L. Cook are gratefully acknowledged. This study was supported by the United States Office of Naval Research.

References

1. M. K. JAIN and A. S. ABHIRAMAN, *J. Mater. Sci.* **22** (1987) 278.
2. M. K. JAIN, M. BALASUBRAMANIAN and A. S. ABHIRAMAN, submitted for publication.
3. M. K. JAIN, PhD thesis, Georgia Institute of Technology, Atlanta, Georgia (1985).
4. L. E. ALEXANDER, "X-ray Diffraction Methods in Polymer Science," (Wiley-Interscience, New York, 1969).
5. M. K. JAIN and A. S. ABHIRAMAN, *J. Mater. Sci.* **18** (1983) 179.
6. S. B. WARNER, D. R. UHLMANN and L. H. PEEBLES Jr, *ibid.* **14** (1979) 1893.
7. S. B. WARNER, L. H. PEEBLES Jr and D. R. UHLMANN, *ibid.* **14** (1975) 565.
8. O. P. BAHL and L. M. MANOCHA, *Fibre Sci. Technol.* **9** (1976) 77.
9. D. J. MULLER, E. FITZER and A. K. FIEDLER, Proceedings of the International Conference on Carbon Fibres, their composites and applications, (Plastics Institute, London 1971) paper 2.
10. E. FITZER and D. J. MULLER, *Die Makromol. Chemie* **144** (1971) 117.
11. E. FITZER and M. HEYN, *Chem. Ind.* **16** (1976) 663.

Received 8 October 1985
and accepted 22 May 1986